JOURNAL OF GEOPHYSICAL RESEARCH, VOL. 96, NO. B6, PAGES 10,145–10,158, JUNE 10, 1991

Reflection Polarity of the Midcrustal Surrency Bright Spot Beneath Southeastern Georgia: Testing the Fluid Hypothesis

THOMAS L. PRATT[1], ERNEST C. HAUSER, THOMAS M. HEARN[2], AND TIMOTHY J. RESTON[3]

Institute for the Study of the Continents, Cornell University, Ithaca, New York

A small reflection seismic experiment with an explosive source was conducted in southeastern Georgia to determine the polarity of an unusually strong midcrustal reflector, the Surrency Bright Spot (SBS), which was found at a depth of approximately 16 km during earlier COCORP profiling in the region. In addition to being very bright, the SBS is notable for being unusually flat and horizontal for about half of its 4 km length. As these characteristics are similar to those of fluid-caused reflections at shallow depths, it has been suggested that the SBS may be caused by in situ midcrustal fluids. If caused by fluid enclosed in fracture porosity in solid rock, the reflection would be expected to exhibit a negative polarity from the top of the porous zone. The vibroseis data, however, gave ambiguous results with regard to polarity due to the limited bandwidth and inherent uncertainties about the phase of the source signal. The new experiment consisted of four dynamite shots, each recorded at three receiver stations by Seismic Group Recorders (SGR) borrowed from Amoco Production Company. Comparison of the dynamite records with geophone polarity tests indicate that the SBS is characterized by a positive reflection coefficient at its top. This result itself does not negate the fluid hypothesis - a fluid-fluid interface could cause the positive reflection as well as the 'flat-spot' nature of the reflector. Waveform modeling shows that the SBS is caused by two or more thinly-spaced reflectors. A relatively high-impedance layer about 120 m thick provided a good match to the observed dynamite data, but requires a lower boundary having a slightly smaller reflection coefficient than the upper boundary (0.7 versus 1.0). A ~150 m thick porous zone model also provided a relatively good fit to the observed dynamite data, but in this model the polarity test requires that the initial SBS reflection (of positive polarity) be caused by a fluid-fluid interface within the porous zone and that the top of the porous zone be relatively non-reflective. Though these observations do not preclude the fluid hypothesis, they certainly make the high-impedance model the simpler of the two alternatives presented here. The additional constraints imposed by the modeling also suggest that the SBS is more complex than these simple, two-interface models. In either of these cases wavelet tuning contributes in part to the unusually large amplitude of the SBS reflection.

INTRODUCTION

A number of unusually bright reflections ('bright spots'), often at midcrustal depths, have been imaged on deep seismic reflection profiles [*Brown et al.*, 1987; *Hyndman and Shearer*, 1989]. These include strong reflectors at depths of 15 km beneath Death Valley, 18-22 km beneath the Rio Grande rift [*deVoogd et al.*, 1988], 9.5 km beneath the Black Forest in Germany [*Luschen et al.*, 1987], and the midcrustal Surrency Bright Spot in the southern Appalachians [*Wille*, 1987]. The Death Valley and Rio Grande bright spots lie within actively rifting hot crust and are interpreted to be due to magma [*Brown et al.*, 1980; *deVoogd et al.*, 1988; *Ake and Sanford*, 1988]. The others, however, lie within cool, stable crust and alternative explanations may therefore be needed. The presence of fluids in porous zones has been advanced as one possible explanation [*Brown et al.*, 1987; *Luschen et al.*, 1987; *Wille*, 1987].

Perhaps the best candidate to date for a middle or lower crustal reflection caused by trapped fluids is the Surrency Bright Spot (SBS), discovered at a depth of 16 km in crystalline basement rocks beneath southeastern Georgia by the Consortium for Continental Reflection Profiling (COCORP) [*Brown et al.*, 1987; *Wille*, 1987] (Figures 1, 2, and 3). In addition to having an amplitude more than 10 dB above background levels on field records, making it by far the strongest reflection in the area and among the strongest yet recorded on COCORP profiles, the SBS is flat and level along about 2 km of its length (Figure 2). The SBS thus has two features, high amplitude and an apparent "flat spot" geometry, which are often diagnostic of a fluid-caused bright spot [*Backus and Chen*, 1975; *Ensley*, 1984]. The SBS has been suggested to lie within the Late Paleozoic suture between African and North American crust as delineated from drillhole data, magnetic data, and the COCORP profiles [*Nelson et al.*, 1985]. In such a geologic setting, fractional and/or metamorphic waters derived from underthrust sedimentary strata could provide a potentially large source of fluids [e.g., *Fyfe*, 1986].

The existence of significant quantities of free fluids in the middle and lower crust has been suggested from several lines of indirect evidence, most noteably the observation of relatively high conductivity in the lower crust [*Gough*, 1986; *MacDonald*, 1988; *Bailey et al.*, 1989; *Hyndman and Shearer*, 1989]. Other authors maintain that fluids cannot explain the observations or are unlikely in the deep crust [*Frost et al.*, 1989; *Yardley*, 1986; *Warner*, 1990]. Unequivocal evidence for midcrustal fluids in at least one locality comes from ultradeep drilling in the Kola peninsula of the Soviet Union where open, fluid-filled fractures to depths of 9 km have been observed [*Kozlovsky*, 1984]. Direct sampling of the lower crust is not practical at present, but magnetotelluric studies in several areas indicate a highly conductive lower crust likely

[1]Now at U.S. Geological Survey, Golden, Colorado.
[2]Now at Department of Physics, New Mexico State University, Las Cruces.
[3]Now at GEOMAR, Kiel, Germany.

Paper number 91JB00766.
0148-0227/91/91JB-00766$05.00

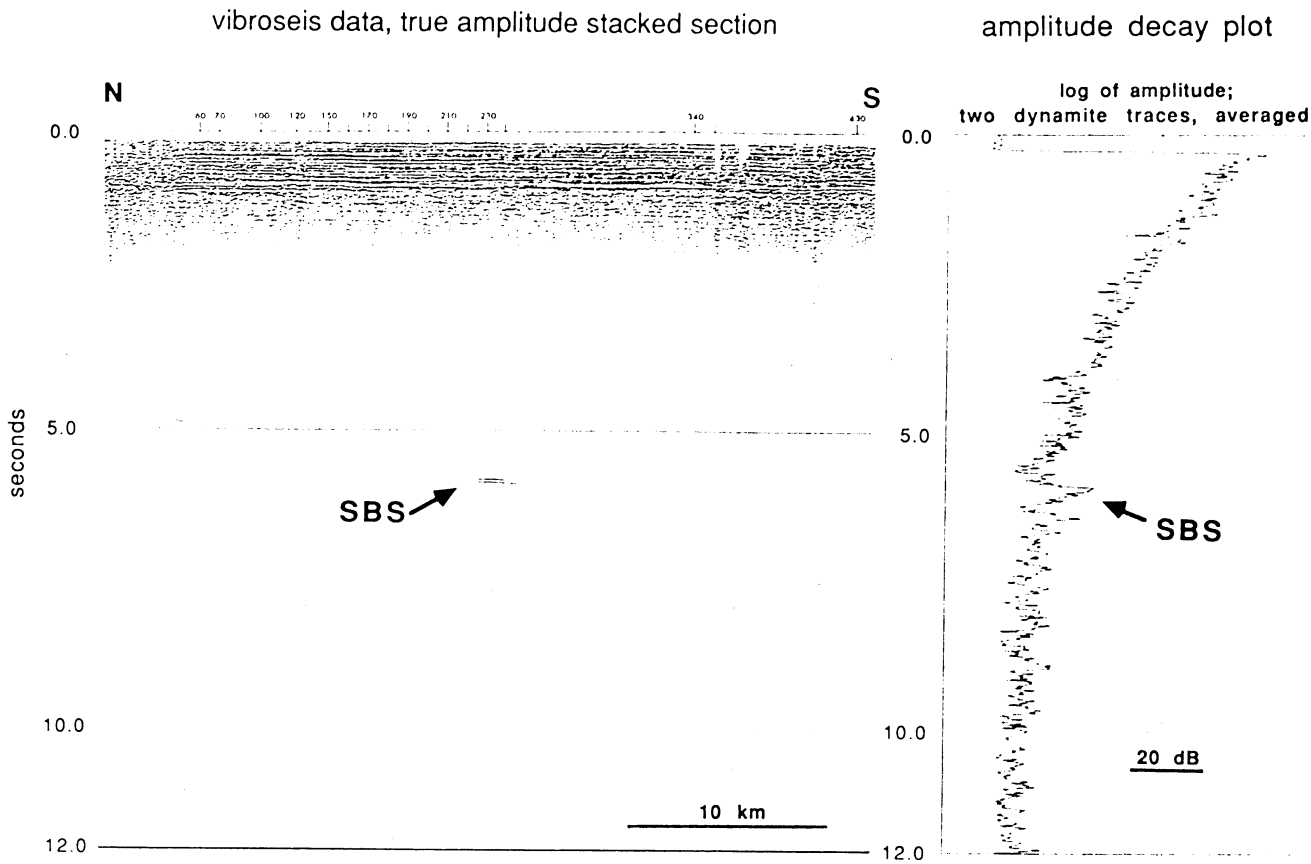

Fig. 1. The Surrency Bright Spot (SBS) as imaged on a true-amplitude version of the original COCORP stacked vibroseis section and on an amplitude decay plot of the dynamite data obtained over the feature. No scaling has been applied to the stacked section; only the shallow Atlantic Coastal Plain strata and the exceptionally strong SBS are visible. The amplitude decay plot shows that the SBS has an amplitude approximately 10 dB above background levels on unstacked records. Seismic section is plotted at a vertical:horizontal ratio of about 1:1 at 6 km/s.

caused by small amounts of interconnected fluid [*Hyndman and Hyndman*, 1968; *Gough*, 1986; *Bailey et al.*, 1989; *Hyndman and Shearer*, 1989], though it has been suggested that graphite films on grain boundaries could also cause the high conductivity layers [*Frost et al.*, 1989; *Shankland*, 1989]. If fluids are present in the deep crust, however, the implications for such diverse geologic issues as the mechanics of the lower crust, the origin and evolution of magmas and metamorphic rocks, and the deposition of ores are substantial [*Fyfe*, 1986].

Seismic reflection studies have renewed the deep-crustal fluid debate because pore fluids are often associated with strong reflections in upper crustal sections [e.g., *Koefoed*, 1955; *Domenico*, 1974] and have therefore been debated as a cause for the prominent reflections widely seen in the lower crust [*Matthews and Cheadle*, 1986; *Hyndman and Shearer*, 1989; *Warner*, 1990]. In addition, the seismic reflection technique has been used successfully to confirm the presence of fluids in the shallow crust [e.g., *Almoghrabi and Lange*, 1986; *Ensley*, 1984; *Robertson and Pritchett*, 1985] and thus provides an opportunity to identify deep crustal fluids in situ. The discovery and verification of a deep crustal reflection caused by fluids is therefore an objective of deep seismic profiling worldwide.

A key test for the fluid hypothesis is reflection polarity on compressional-wave seismic data. Fluid-caused reflectors contrast with most other likely alternatives in that increased porosity generally causes a velocity and density decrease [e.g., *Koefoed*, 1955; *Gardner et al.*, 1974; *Gregory*, 1976; *Carlson and Herrick*, 1990; *Hyndman and Shearer*, 1989]; porous zones are thus usually characterized by a negative reflection coefficient at the top of the zone and a positive coefficient at the base. A gravitationally-controlled fluid-fluid boundary may cause an additional reflection with a subhorizontal attitude and positive polarity within the porous zone. The result is a complex package of several closely-spaced interfaces (top of porous zone, fluid boundary, bottom of porous zone) rather than just a single boundary or a double interface surrounding a thin body of material [*Backus and Chen*, 1975; *Ensley*, 1984]. Unfortunately, vibrator sources like those used in the original COCORP survey produce a source wavelet which is not impulsive and whose phase characteristics (polarity) are difficult to determine because of the complexity of the vibroseis system and its interaction with the ground. The relatively narrow bandwidth (8-32 Hz) used in the original reconnaissance COCORP survey also produced a correspondingly broad source wavelet which could limit the resolution of any interfaces within the SBS. Determinations of the polarity or detailed geometry of the SBS using the original COCORP data have therefore been inconclusive.

A small seismic reflection experiment with an explosive source was carried out over the SBS in late 1989 to test the fluid hypothesis by determining the reflection polarity and providing a broader range of source frequencies and thus a higher resolution image of the SBS. In addition, receivers to the side of the main

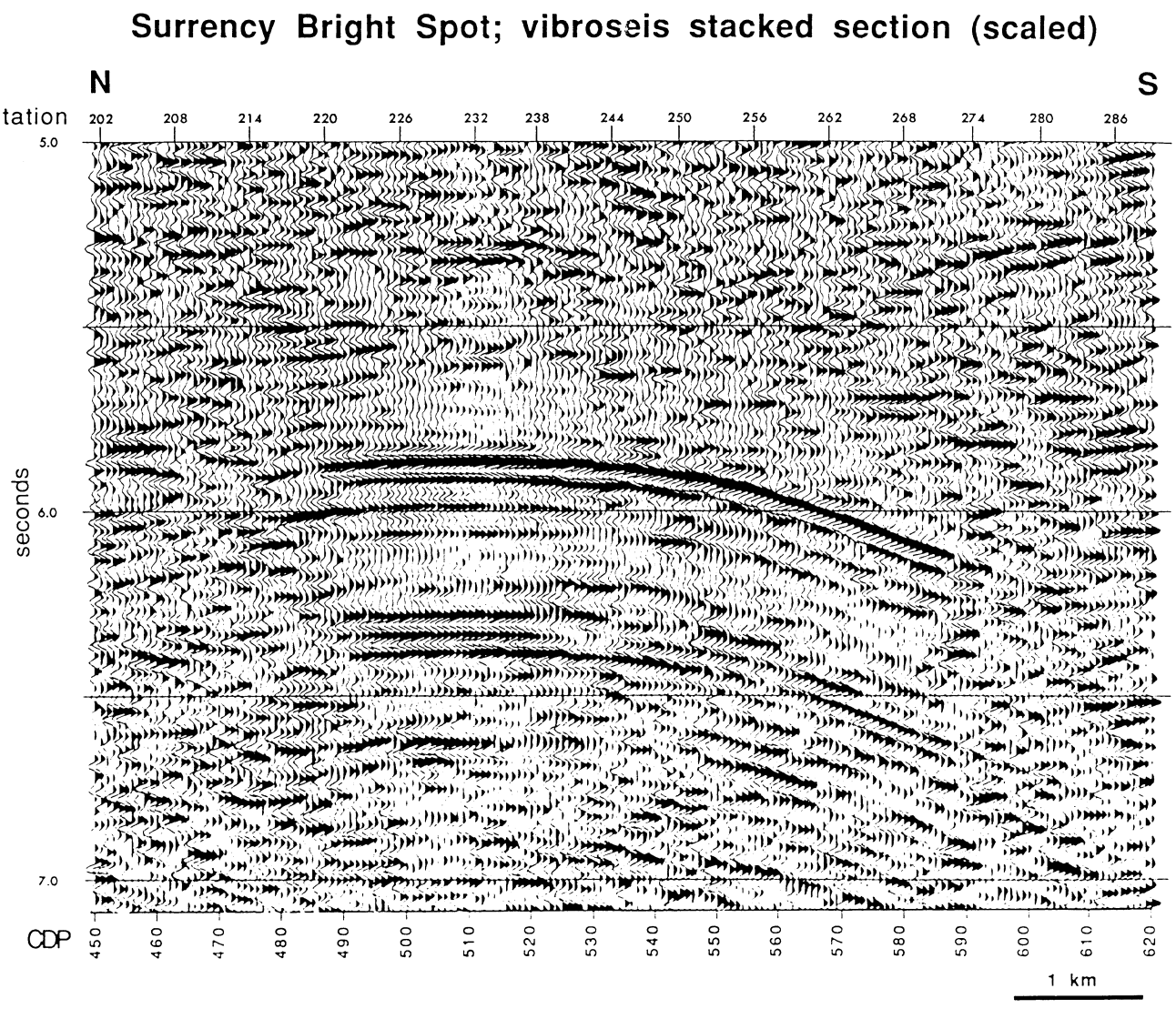

Fig. 2. Detail of the Surrency Bright Spot (SBS) on the vibroseis stacked section after the application of automatic gain control (AGC). Note the nearly 2.0 km long level portion at the northern half of the SBS and the apparent diffraction tail to the south. The reflection lying approximately 0.5 s below the SBS is believed to be caused by multiply-reflected energy within the near surface sedimentary rocks. Section is plotted at a vertical:horizontal ratio of about 1:1 at 6 km/s.

profile were used to estimate the attitude of the SBS perpendicular to the original profile. The results of this experiment, described herein, place severe constraints on the cause of the SBS reflection. Though the results do not prove or disprove the fluid hypothesis, they force the fluid model to be complex in comparison to the much simpler mafic sill or ultramafic body model.

Data Collection And Processing

Field conditions for the experiment were almost ideal. The surrounding countryside is flat and comprises large tracts of timber with no structures or habitations within the experiment area. Station locations from the original COCORP profile along a straight north-south dirt road were resurveyed and used during the experiment (Figure 3). The SBS lies beneath the intersection of this north-south dirt road, having little or no traffic, and a paved highway (U. S. Route 341) carrying moderate traffic (Figure 3). Also in the area is a powerline and a lightly-used railroad track which the highway crosses on an overpass. Passive recording the day before the experiment showed that the overpass was a major source of low-frequency noise when vibrations were induced by traffic or wind, and recorders were therefore situated away from that structure as well as the powerline (Figures 3 and 4). Winds were very light during the recording, and detonation of shots was held until no traffic was in sight on the roads.

Instrumentation included six Seismic Group Recorders (SGRs), 10Hz geophones, a field control unit, and a microcomputer system borrowed from the Amoco Production Company, Tulsa research facility. In addition, a Nimbus 6-channel analog recording system with single-element geophones and 4 MEQ-800 portable drum recorders were used for monitoring and noise tests. A day was spent passively monitoring with both the MEQ and SGR instruments to determine ambient noise levels at different locations in the area at different times of day. It was during these tests that noise from the powerlines and overpass was measured and the locations of the recorders modified accordingly.

Three of the recorders were deployed in a line along the original COCORP profile while two other recorders were placed

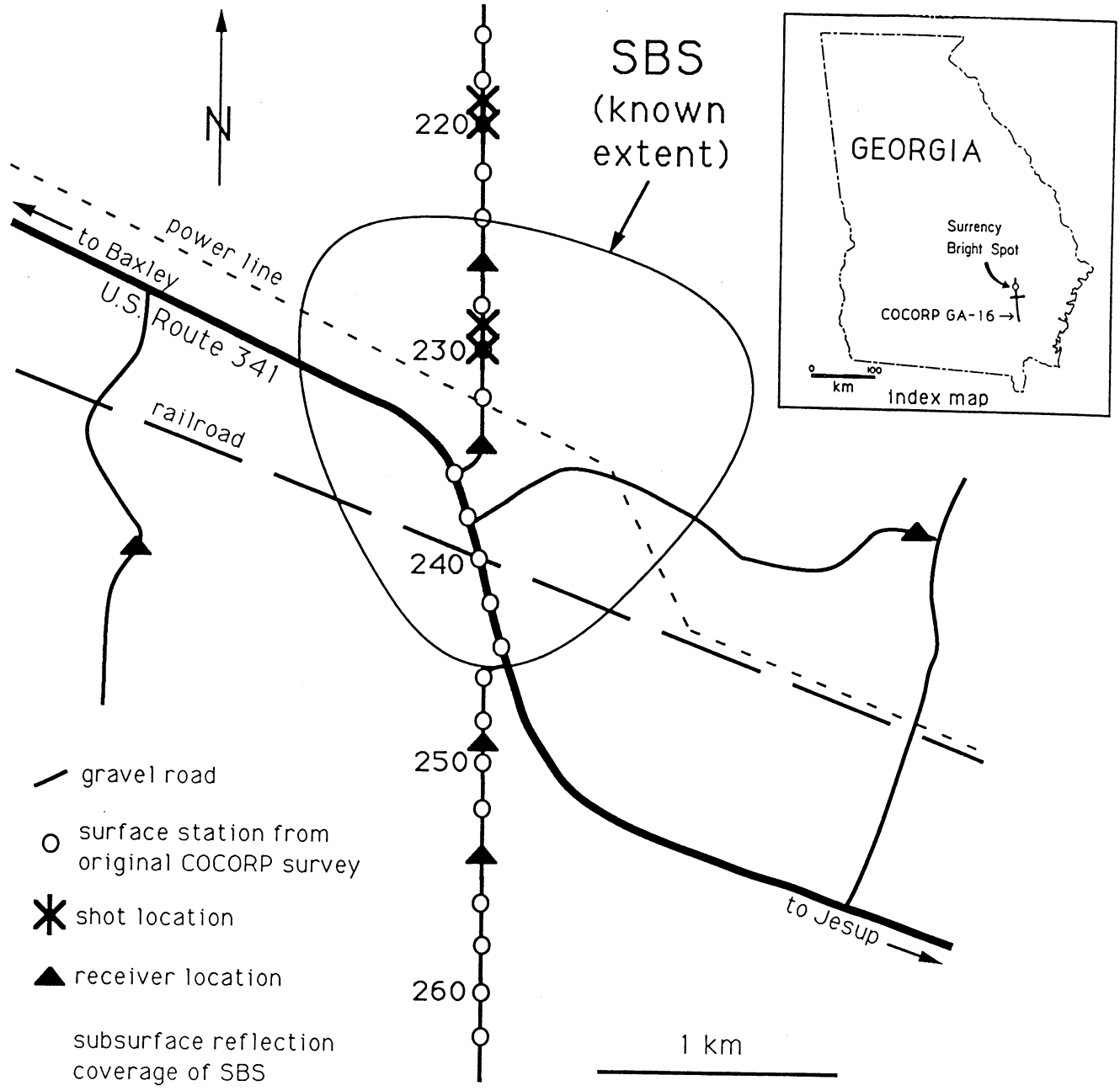

Fig. 3. Map of the experiment area showing the station locations from the original COCORP survey (re-used during the dynamite experiment), the locations of the dynamite shots (asterisks), and the receiver locations (triangles). The shading shows the location of the reflection points which have imaged the relatively flat portion of the SBS; the enclosure shows the approximate minimum extent of the relatively flat portion of the SBS.

approximately 1.5 km to each side of the main profile (Figure 3). The final SGR was needed to trigger the explosives and was not available for recording. The in-line receivers were placed at stations 226, 234, and 249 for sources at stations 229 and 230, and at stations 234, 249, and 254 for sources at stations 219 and 220. These locations were chosen to maximize the reflection point coverage on the flat portion of the bright spot while avoiding the noise associated with the powerlines and overpass (Figure 4). A 12-element linear, 91.5 m (300 ft) receiver array pointed toward the shots was used at all stations.

Shot holes were drilled at stations 219, 220, 229 and 230 to a depth of 19 m (62 ft) and cased with 6" PVC to prevent collapse in the soft sediments. Water was encountered within one meter of the surface. Dynamite (Petrogel) charges consisting of 11.4 kg (25 lbs) at station 230, 18.2 kg (40 lbs) at stations 229 and 220, and 20.5 kg (45 lbs) at station 219 were placed in the lower 7 m of the holes and tamped with coarse sand. The shots were detonated in order of decreasing station number (station 230 first, station 219 last) after pausing between the second and third shots to move the one recorder from station 226 to station 254. Shots 220 and 219 apparently had the best energy coupling because they produced the strongest reflections; shot 220 was the best tamped and was the only shot which did not eject some casing from the shot hole.

The traces from the new experiment underwent effectively the same processing as the original COCORP survey except that filter and deconvolution were omitted to keep the wavelet free from

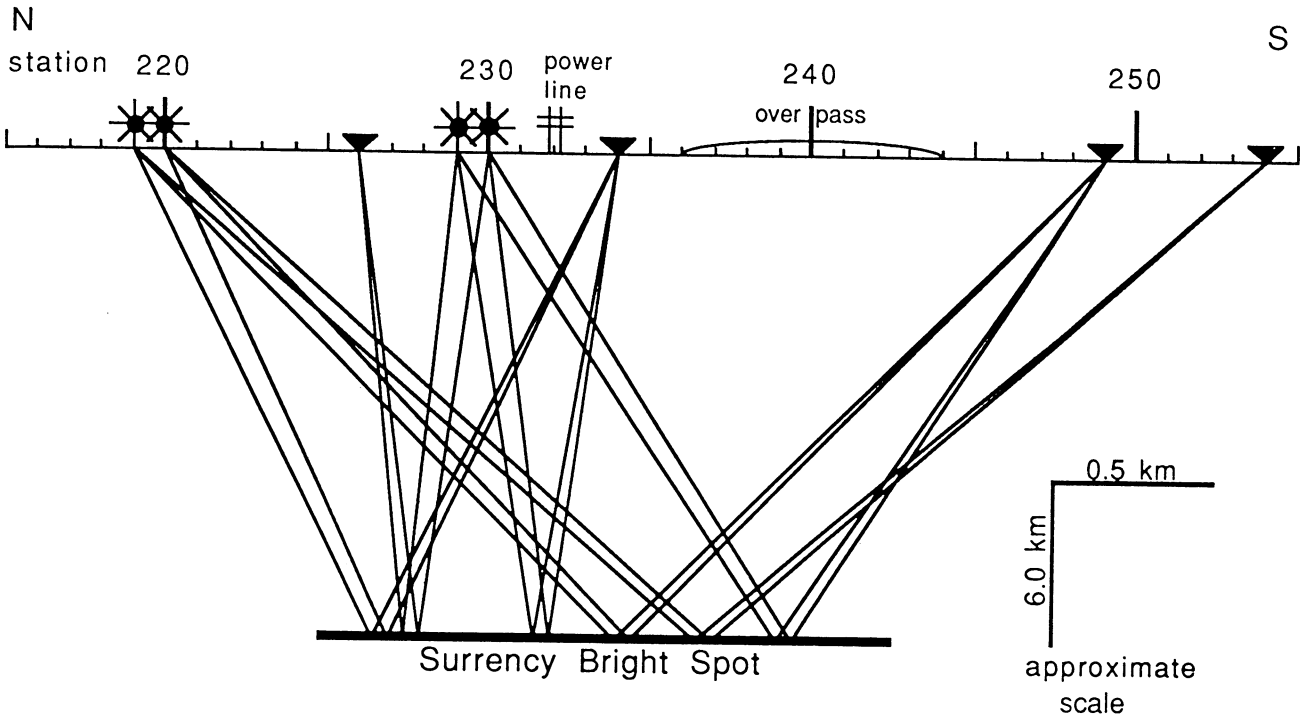

Fig. 4. Diagram of the reflection point coverage of the dynamite experiment along the main north-south profile over the SBS. Receiver locations are shown as triangles, shot locations are shown as asterisks, and the raypaths are shown as straight lines. The source and receiver locations were chosen to maximize the subsurface coverage of the SBS while avoiding the noise associated with the powerline and road overpass.

distortion. Stretching due to the normal moveout correction is very small given the large travel time and small source-receiver offsets and therefore produces a negligible change in the wavelet shape. The single-fold dynamite traces were then gathered into common depth points (CDPs) for comparison with the same CDP traces from the stacked vibroseis section. The corresponding single-fold vibroseis traces were not used in the final analysis because they have a considerably lower signal-to-noise ratio than the dynamite records, yielding an inconsistent wavelet shape that is difficult to determine on the records. Datum static corrections were computed using the true (subsurface) locations for the shots, and thus include the uphole corrections. Surface-consistent static corrections of up to 12 ms were applied to the dynamite data to align the reflection across the suite of traces. To make the sampling consistent with the dynamite data, the vibroseis traces, originally recorded at an 8 ms sample rate, were resampled at 2 ms using a cubic spline interpolation routine [*Akima*, 1970].

RESULTS

Travel Time and Attitude

The SBS is seen on the dynamite records (Figure 5) as a strong reflection package between 5.8 and 6.0 s two-way travel time after normal moveout. Data from the west side station, located approximately 1.5 km west of the main profile (Figure 3), suggest that the SBS reflector occurs at traveltimes approximately 30 ms later to the west (dashed lines, Figure 6). This either indicates a westward dip of 6° or 7° (assuming a velocity of 5800 m/s) for the SBS or that we are imaging part of a diffraction from the edge of the SBS at the side station. Most importantly, the reflections recorded at the west side station demonstrate that the SBS is a nearly horizontal body in the midcrust and is not due to sideswipe from a reflector located in the shallow crust a significant distance to the side of the COCORP line.

In contrast, traces recorded at the station 2 km east of the main profile suggest that the SBS has changed character at the CDP points about 1.0 km east of the main line (Figure 6). Large-amplitude reflections are imaged there, but their onset on the southern profile may be occuring at about 5.75 s, or about 100 ms earlier than on the main line. On the northern profile the wavelet shape is again different from that on the main line and it appears to have the opposite polarity. One suggestion is that the SBS increases in complexity, forming several layers of varying thickness east of the main profile. Future work will include a crossline which should resolve this issue.

Assuming that the same or related reflectors are being imaged on all of these data, a minimum size can be estimated for the SBS. The SBS has an E-W width in excess of 1.75 km and a N-S dimension (from the original COCORP profile) of approximately 2.0 km (for the flat region, not including the dipping portion). This translates into an area of about 3 km^2 (Figure 3). The SBS thus has a minimum size whose diameter is about half that of the fresnel zone for our dynamite sources.

Polarity

A polarity test was carried out to associate geophone motion with the recorded polarity. The test was conducted by mounting all 12 geophones of a receiver channel on a small board and striking the board firmly from the bottom so that it was lifted. This motion moves the geophones upward and is equivalent to an upward motion of the ground. In all repetitions of the test, a sharp negative (leftward) deflection was recorded by the SGR at the

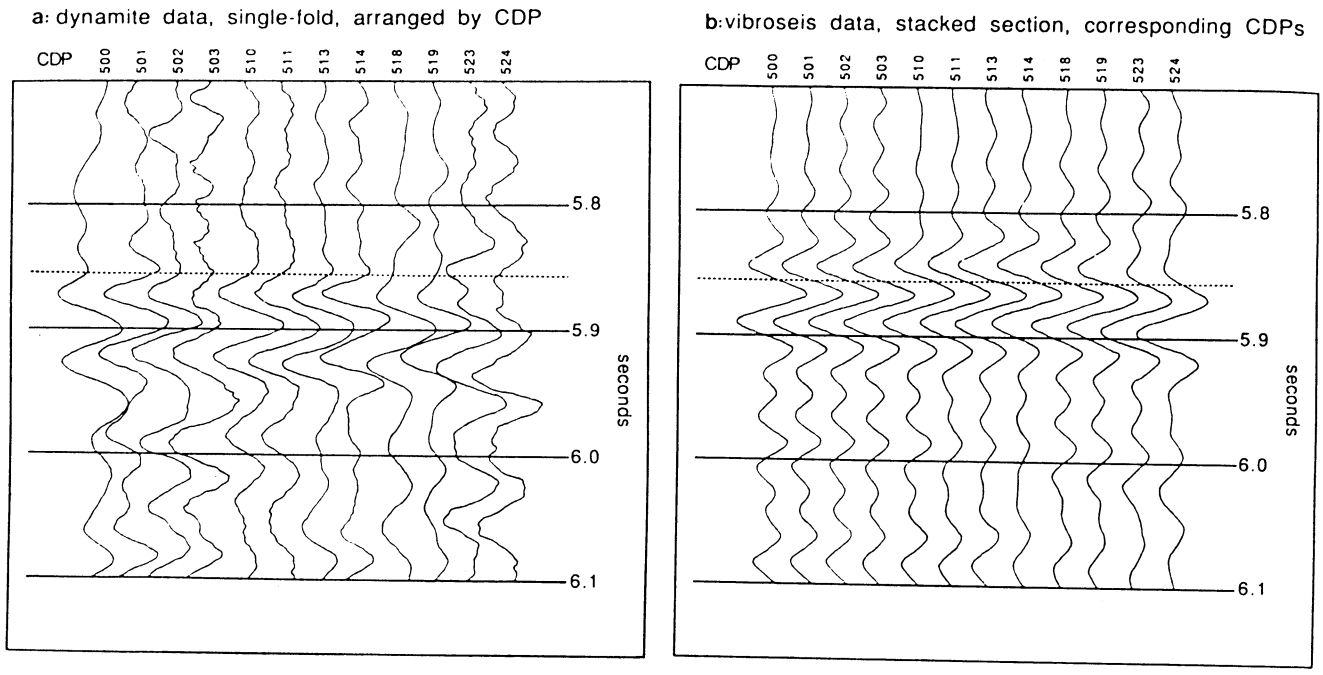

Fig. 5. (*a*) Single-fold field records from the dynamite experiment along the main north-south profile, arranged by common-depth-point (CDP). (*b*) Equivalent CDP traces taken from the stacked vibroseis section. The dashed line at approximately 5.86 s is the onset of the SBS reflection package as interpreted from the dynamite data. Note the leftward deflection of the dynamite traces at this time. Traces are scaled to equalize the maximum amplitude of each trace.

onset of motion (Figure 7), thus indicating that negative (left) corresponds to upward geophone motion.

The first refracted arrivals also move the geophone upward and therefore provide an independent check of the polarity test. Confirming the test, all but one of the recorded traces showed an impulsive, negative first (refracted) arrival (Figure 8); the one exception had an emergent, and therefore ambiguous first break. Both the tap test and first breaks establish that negative trace amplitudes are associated with upward geophone motion. All of the data within this paper are plotted with a negative deflection to the left, representing an upward geophone motion on the dynamite data. The vibroseis data, because of uncertainties in the phase of

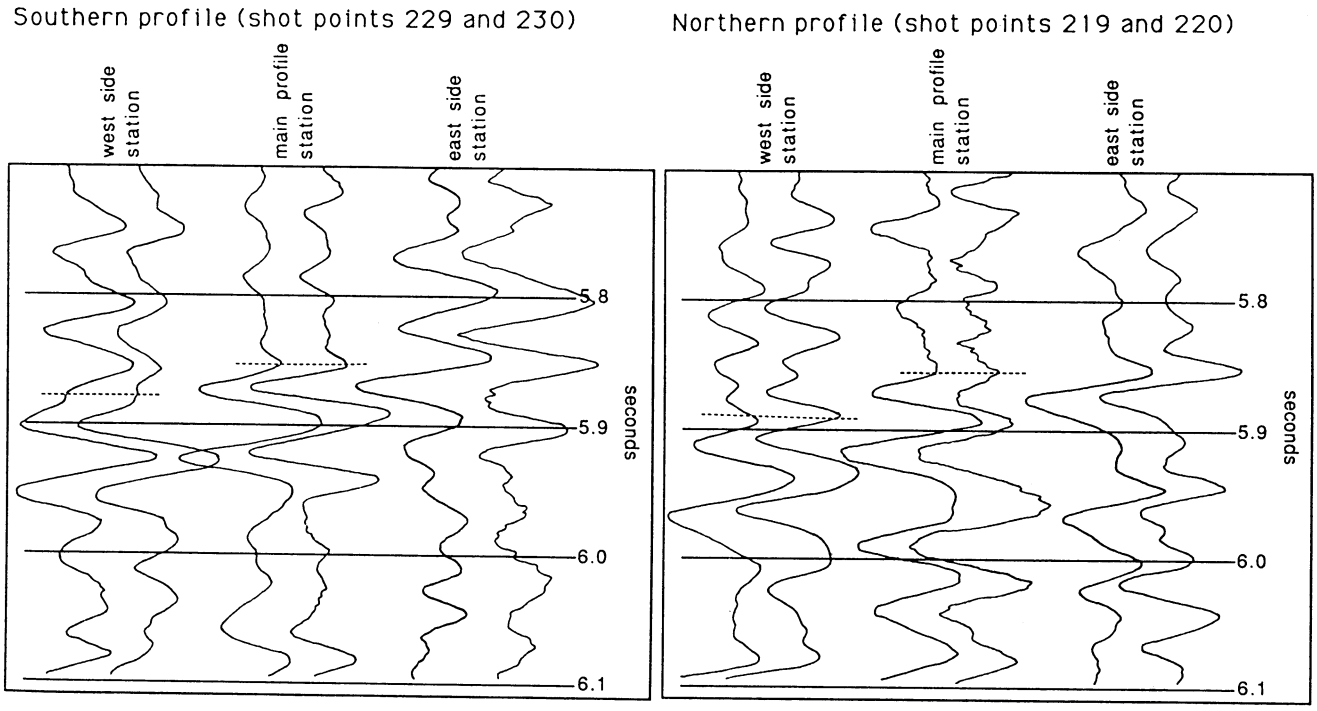

Fig. 6. Pairs of traces from the northern and southern pairs of shots recorded at the west side station (left), the main north-south profile (center), and the east side station (right). The west side station shows a reflection package similar to that on the main profile but arriving slightly later; the east side station shows a different character for the SBS reflection. Traces are scaled to equalize the maximum amplitude of each trace.

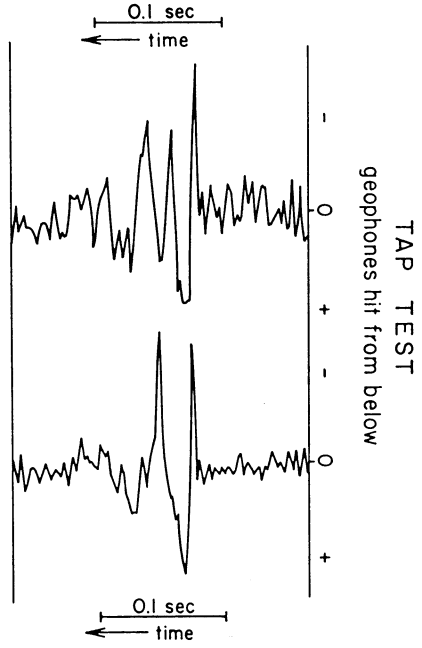

Fig. 7. Recordings from two of several repeated geophone tap tests. All geophones from one receiver channel were mounted on a board which was then struck from the bottom to simulate upward ground motion. Note the strong leftward (negative) deflection of the traces at the onset of motion. Traces are scaled to equalize the maximum amplitude of each trace.

the source signal, are of unknown polarity and the plot direction is therefore incidental.

The SBS reflection package is initiated (dashed line in Figure 5) by a negative deflection, the onset of which interrupts the preceding ground motion. Note that CDPs 523 and 524 (Figure 5) have a slightly later arrival time for the SBS because they are on the sloping portion of the SBS reflection (Figure 2). This negative deflection indicates an upward ground motion and hence a positive reflection coefficient at or near the top of the SBS. This in turn requires a velocity and/or density increase with depth across the reflector. The most straightforward conclusion, therefore, is that the SBS is caused by a high-impedance (high velocity or density) body such as a mafic sill or an ultramafic body rather than a fluid.

A dense or high-velocity material would obviously be marked by a positive reflection at its upper surface; however, the positive reflection polarity for the top of the SBS does not necessarily preclude fluids as a cause. A fluid-fluid boundary within a porous zone could also produce an initial positive reflection if the top of the porous zone is nonreflective. For example, a gradual increase in porosity with depth at the top of the porous zone may not produce a significant reflection, but the interface between two fluids of different densities within the porous zone could. This is, in fact, the scenario implied by the "flat-spot" analogy [*Backus and Chen*, 1975; *Ensley*, 1984]. Modeling of the SBS was undertaken to assess these alternatives.

Modeling

To determine the minimum number and polarity of the interfaces present at the SBS, waveform modeling was undertaken. The shape of the source wavelet on the dynamite data was assumed for modeling purposes to be minimum-phase [*Robinson and Treitel*, 1980]. This assumption is justified because the impulsive source signal from explosive sources is generally thought to be minimum-phase [*White and O'Brien*, 1974] and any reverberations, multiples, or free-surface ghosts caused by the overlying strata (Atlantic Coastal Plain sedimentary rocks) produce 'spike trains' which are also minimum phase [*Robinson and Treitel*, 1980, chap. 11 and appendix 13-1]. The convolution of these two signals should therefore produce a minimum-phase source wavelet which includes the complexities introduced by reverberations and ghosts.

The minimum-phase wavelets (Figure 9*a*) were extracted from the 5.0-7.0 sec portion of each dynamite trace using the Kolmogoroff method of spectral factorization [e.g., *Claerbout*,

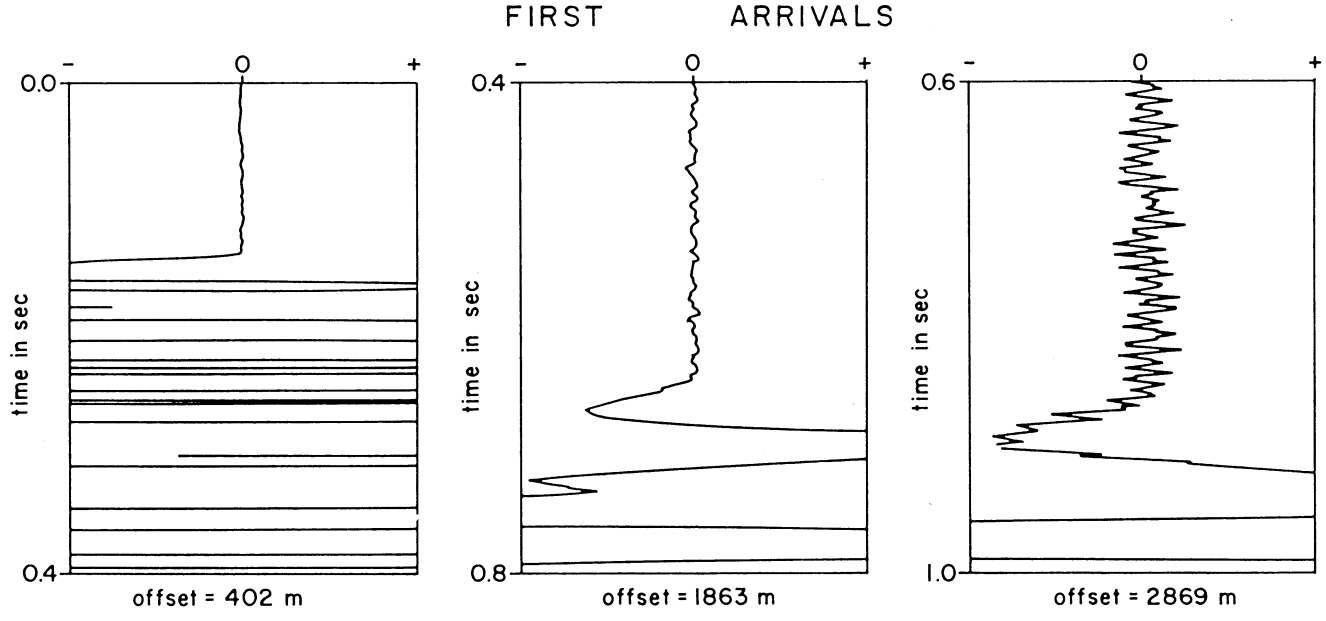

Fig. 8. Field records showing the first (refracted) arrivals at several receivers with differing source-receiver offsets. The impulsive arrival corresponding to the first motion (ground moving upward in response to a refracted arrival) show a leftward (negative) deflection on all traces with an identifiable first motion, consistent with the tap test. The gain levels are different for each trace in this plot, thus making the noise levels appear to vary.

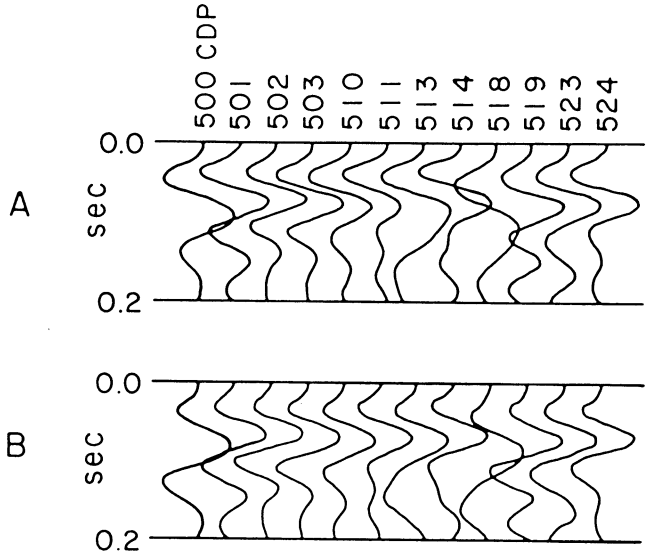

Fig. 9. (*a*) The minimum-phase wavelets extracted from the dynamite data. (*b*) The geophone compensated versions of the wavelets used in the modeling. The 12 wavelets correspond to the 12 recorded traces shown in Figure 5.

1976; *Yilmaz*, 1987, appendix B-4]. The wavelets used for modeling the corresponding vibroseis traces were simply computed from the autocorrelation function of the vibroseis data under a zero-phase assumption. To suppress the high-frequency components introduced by windowing during the factorization process, all of the extracted wavelets used in the modeling were 'smoothed' slightly by applying a zero-phase, 4-40 Hz band-pass filter. Because these source wavelets are factored from the data, they include any reverberations or 'ghosts' present in the field records (note that the apparent multiple seen on Figure 2 about 0.5 s below the SBS occurs at about 0.5 s on the wavelet, far below any of the plots shown here).

Using the autocorrelation function to extract the wavelets is done under the assumption that the amplitude spectrum of the reflectivity series is white (the reflection coefficients have a random amplitude and time distribution) and thus the amplitude spectra of the seismic trace and seismic wavelet are scaled copies of each other. Though this is the basic tenet of predictive filtering and has been found quite robust over years of usage, there is the question here of whether the high-amplitude SBS, which may have an anomalous frequency spectrum because of interfering wavelets, dominates the autocorrelation function and therefore gives an incorrect wavelet after spectral factorization. Figure 10*a* shows the minimum phase wavelet factored from selected 2 s time windows of one trace; note that the wavelet factored from the 2.0 to 4.0 s portions of the seismic traces (i.e., preceeding the SBS) is virtually identical to the wavelet factored from the 5.0-7.0 s portion of the trace (i.e., including the SBS). The similarity of the wavelets from the 2.0-4.0 s and the 5.0-7.0 s portions of the traces is an important step in justifying our modeling procedure; it shows that the SBS, even with its large amplitude, does not significantly alter the amplitude spectrum of the data and thus the wavelet shape. In short, the "white" reflectivity series assumption is acceptable for our modeling.

In addition to the source wavelet and the reflectivity function, other effects which need to be considered in the modeling are the receiver array, geophone response, and instrument response. The final trace is the convolution of these response functions with the source wavelet and reflectivity:

$$\text{trace}(t) = \text{source}(t)*\text{reflectivity}(t)*\text{geophone}(t) *\text{receiver array}(t)*\text{instrument}(t)$$

where the asterisk denotes convolution. Because we factored the model source wavelets directly from the seismic trace, the effects of each of these filters are already included in their amplitude spectrum; the issue we need to address here is whether the phase spectrum of the (assumed) initially minimum-phase source wavelet has been altered by the recording apparatus (geophone, receiver arrays, instruments). In particular, if any of these recording effects do not have a minimum-phase response, we need to modify the model wavelets accordingly.

The geophone arrays and recording instruments should have no effect on the phase spectrum of the SBS reflection. Given the large depth of the SBS relative to the source-receiver offsets in the experiment, energy reflected from the SBS arrived at the recorders essentially as vertically travelling waves (i.e., infinite wavelength in the array direction) and the linear receiver arrays should therefore have a negligible effect on the amplitude and phase spectrum of the recorded signal. The recording units (SGR IV group recorders) were digital with an analog antialias filter whose application begins at frequencies (125 Hz and higher for our 250 Hz Nyquist frequency) well above the range of our recordings (0-80 Hz); neither the instrument nor the filter should introduce any phase distortion into the signal.

The phase response of the geophones were taken into account by filtering the model source wavelets with a 'geophone' filter. The geophones were 10Hz vertical phones whose phase characteristics are shown in Figure 11, derived from the general equation for a damped harmonic oscillator:

$$\text{Phi} = 180° - \tan^{-1}[2Df_n f/(f_n^2 - f^2)]$$

where D is percent damping (0.67), f is frequency, and f_n is natural frequency of the geophone (10 Hz). A digital filter with this phase response was applied to the wavelets in Figure 9*a* to produce the wavelets used in the modeling (Figure 9*b*). These model wavelets should thus include the phase effects of the recording system.

An interesting result from the factorization process used to derive the wavelets is the change in wavelet shape and frequency content with traveltime (Figure 10*a*). The wavelet begins (0.0-2.0 s) as a sharp, double-lobed wavelet but quickly broadens as it propagates. Note, however, that below 2.0 s traveltime the wavelet effectively has a constant shape (again compare the 2.0-4.0 s and the 5.0-7.0 s wavelets). This signifies that most of the attenuation is occurring in the shallow portions of the section (the Cenezoic/Mesozoic Atlantic Coastal Plain) whereas the crystalline basement rocks are seismically efficient. Frequency spectra (Figure 10*b*) show that most of the energy above 36 Hz is attenuated before 2.0 s travel time, again suggesting that the higher frequency components do not reach the middle and lower crust. Though the dynamite source was rich in frequencies up to 80 Hz (0.0-2.0 s spectrum in Figure 10*b*), the SBS is illuminated by about the same bandwidth as used in the original vibroseis sweep (8-32 Hz) and the resulting image shows little or no improvement in resolution over the vibroseis image (Figure 5). This loss in frequency content with time prohibited us from using a wavelet from a reflection (or refracted arrival) in the upper portion of the trace to model a deep event like

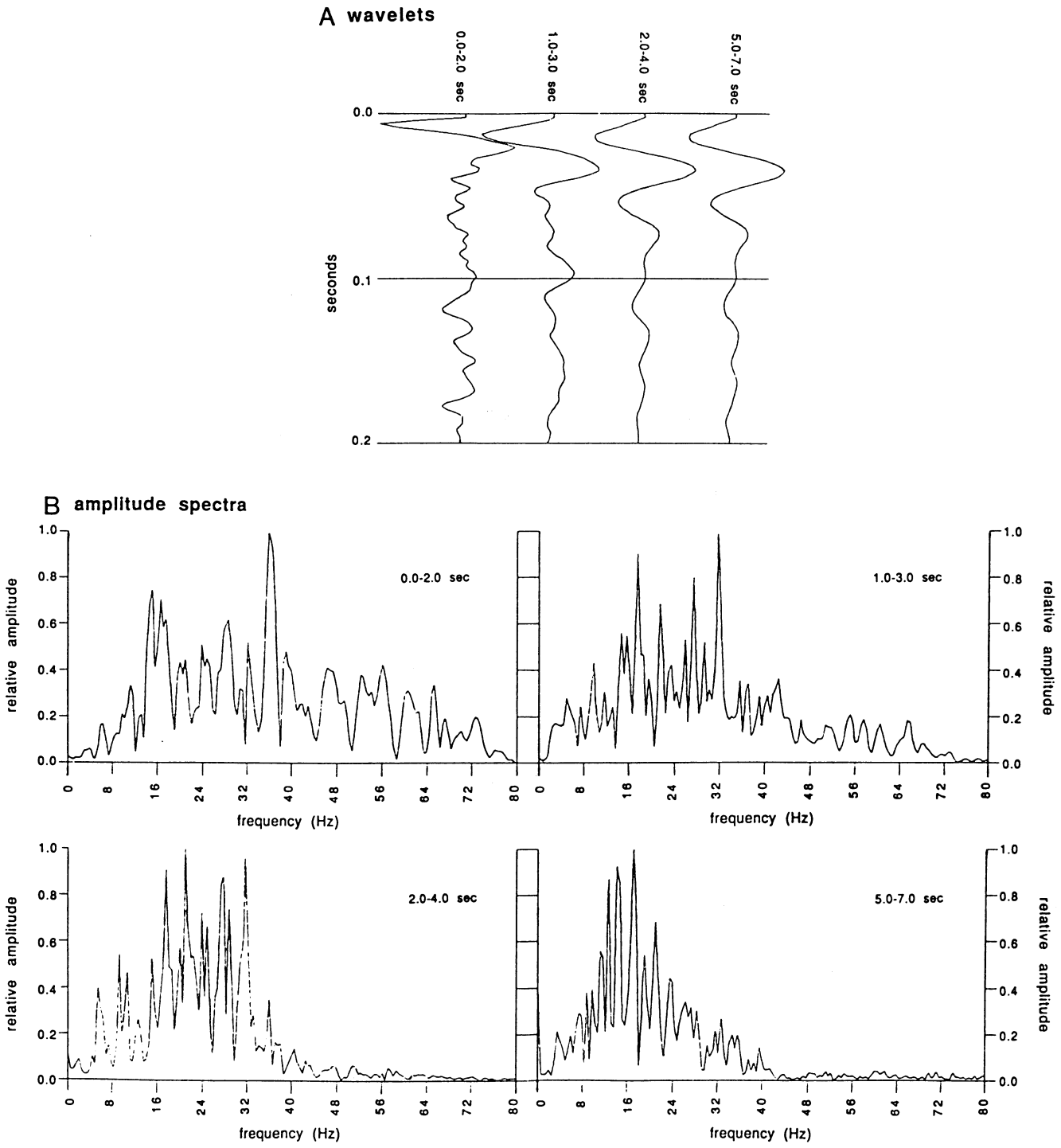

Fig. 10. (*a*) Seismic wavelets and (*b*) corresponding amplitude spectra from selected time windows from one trace of the dynamite experiment. Note that the pulse begins as a sharp wavelet with a broad frequency spectrum (0.0-2.0 s window) but quickly broadens as the higher frequencies are attenuated. Most of the attenuation appears to be occurring in the upper 2.0 s of travel time. The wavelets were extracted from the seismic traces using the Kolmogoroff method of spectral factorization [*Claerbout*, 1976].

the SBS, as others have done elsewhere [e.g., *Goodwin et al.*, 1989].

The wavelets derived from the dynamite (Figure 9*b*) and stacked vibroseis traces (the autocorrelation function) were convolved with suites of impulse response models (synthetic spike trains) which simulate (Figure 12, bottom): (1) a single interface; (2) a thin, high-impedance (high velocity or density) layer; (3) a fluid model with equal reflection coefficients at the top and bottom of the lower fluid zone; and (4) a fluid model with the base of the lower fluid zone having a reflection coefficient half that of the top.

The upper reflector in each model, of positive amplitude as per the polarity test, was placed so as to align the initial lobes of the synthetic SBS reflection with that on the observed data (Figure 12). In the case of the three latter models the time between the interfaces (*dt* in Figure 12, bottom) was varied in 10 ms increments to simulate different layer thicknesses. The results for

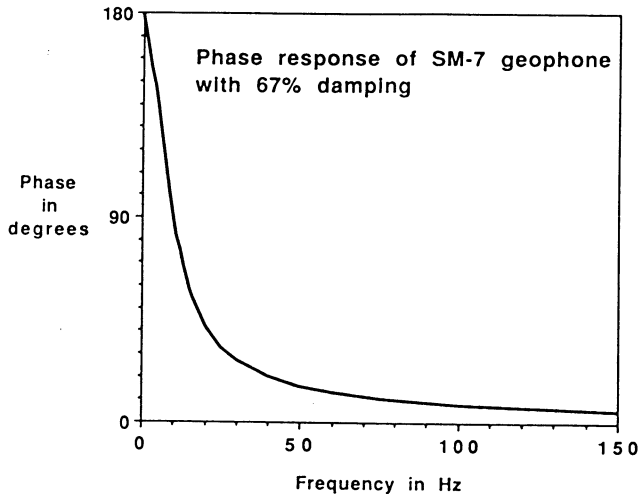

Fig. 11. Phase response of the geophones used in the experiment plotted as a function of frequency.

four of the CDPs are shown in Figure 12 with the observed dynamite trace on the left and the synthetic traces to the right.

The single-interface model produces a reflection of significantly shorter duration than on the field data (Figure 12), suggesting that the SBS is composed of more than one interface. This is not suprising: the limited lateral extent of the SBS reflector requires that it be a relatively small body rather than a half-space, which in turn requires a lower boundary to be present.

The high-impedance models, which have a second reflector with a negative polarity but equal amplitude at time *dt* below the inital positive reflector (Figure 12, bottom), clearly show that any such layer must be between 30 and 40 ms two-way transit time to produce the proper lobe spacing to match the SBS (Figure 12). Thicker layers (50 ms in Figure 12) begin to form a more complex wavelet package than is observed from the SBS while thinner layers (10 to 20 ms in Figure 12) are of too short a duration. These simple high-impedance models, though they match the lobe spacing of the observed data, suffer from having too small an amplitude on the first lobes of the reflection packets. This can be corrected to a large extent by reducing the amplitude of the second (negative) reflection coefficient to 0.7 (high-impedance model in Figure 13), though this complicates the model by implying that either the materials overlying and underlying the SBS are different or, more likely, the SBS is more complex than this simple model implies. For example, the base of the SBS could be less pronounced than its upper surface because the SBS is a tectonically emplaced ultramafic body whose lower boundary has been deformed or abuts against a shear zone rather than the undeformed surrounding country rock. Another scenario is that the SBS is actually composed of two or more thin layers, the uppermost being the strongest reflector. Though not a comprehensive search, our model with the closest match to the dynamite data has a 36 ms reflector separation (about 120 m layer thickness for v=6.8 km/s) with an upper reflection coefficient of 1.0 and a lower coefficient of 0.7 (Figure 13). This model also produces a satisfactory match with the stacked vibroseis data (Figure 13). The high-impedance model thus seems plausible, though perhaps oversimplified.

Fluid model 1, which consists of two equal-amplitude positive reflectors, does not produce an adequate match because its reflection package is of too short a duration, has a more complex waveform, or the later lobes are much larger than on the observed SBS reflection (Figure 12). This result is also not surprising because the amplitudes of the reflections from the fluid-fluid interface and the base of the porous zone are controlled by different physical properties. It therefore would have been fortuitous if these two reflections had the same amplitude.

Fluid model 2, with a lower reflection coefficient 0.5 times that of the upper and both of positive polarity, produces an adequate match when the interface separation reaches about 50-60 ms two-way traveltime (layer thickness of about 140-165 m for v=5.5 km/s; Figure 12). Thicker layers produce a more complex wavelet package than is observed. Our best match with the dynamite data for this model was produced with a lower reflector whose arrival was 54 ms later than that of the upper reflector (fluid model in Figure 13). On this model, the duration and amplitudes of the wavelets are comparable to that of the observed SBS reflection package, though the inconsistent shape to the later parts of the reflection (Figure 13) again suggest that the model is oversimplified; because of the inconsistent shape, we suggest that the high-impedance layer produces a slightly better match to the observed dynamite data. The fit to the vibroseis data for fluid model 2 seems a bit better than the high-impedance model because the amplitude of the later lobes is in better agreement with the observed data (Figure 13); however, the vibroseis data do not seem to be as sensitive as the dynamite data to variations in the reflector geometry. As with the high-impedance model, the fluid model seems plausible but oversimplified.

In summary, a thin, high-impedance model and a simple fluid model both provide plausible explanations for all of the SBS observations to date, but both require a departure from the expected geometry. The high-impedance model must have about a 36 ms reflector separation but does not have equal reflection coefficients at the top and bottom of the body; the fluid model needs about a 54 ms reflector separation, must have a relatively non-reflective top to the porous zone, and must involve more than one fluid.

DISCUSSION

We feel that the high-impedance model provides the more likely explanation for the SBS. Reasonable velocity (v) and density (rho) values for a mafic or ultramafic body could produce a bright reflection. For example, the following model contains two reflection coefficients of 0.1:

$v = 6100$ m/s rho $= 2.7$ g/cm^3

_____ ref. coef $= 0.1$

$v = 6800$ m/s rho $= 3.0$ g/cm^3

_____ ref. coef $= -0.1$

$v = 6100$ m/s rho $= 2.7$ g/cm^3

Assuming a velocity of 6800 m/s, a layer with a two-way transit time of 36 ms (our best model) corresponds to a layer approximately 120 m in thickness. These velocities and densities could represent such typical materials as a mafic dike between granitic gneisses; larger reflection coefficients are possible with other likely rock types, particularly ultramafic rocks [*Hurich and Smithson*, 1987]. The paired positive-negative reflections in the model are well positioned for constructive interference between the top and bottom reflection on both the dynamite and stacked

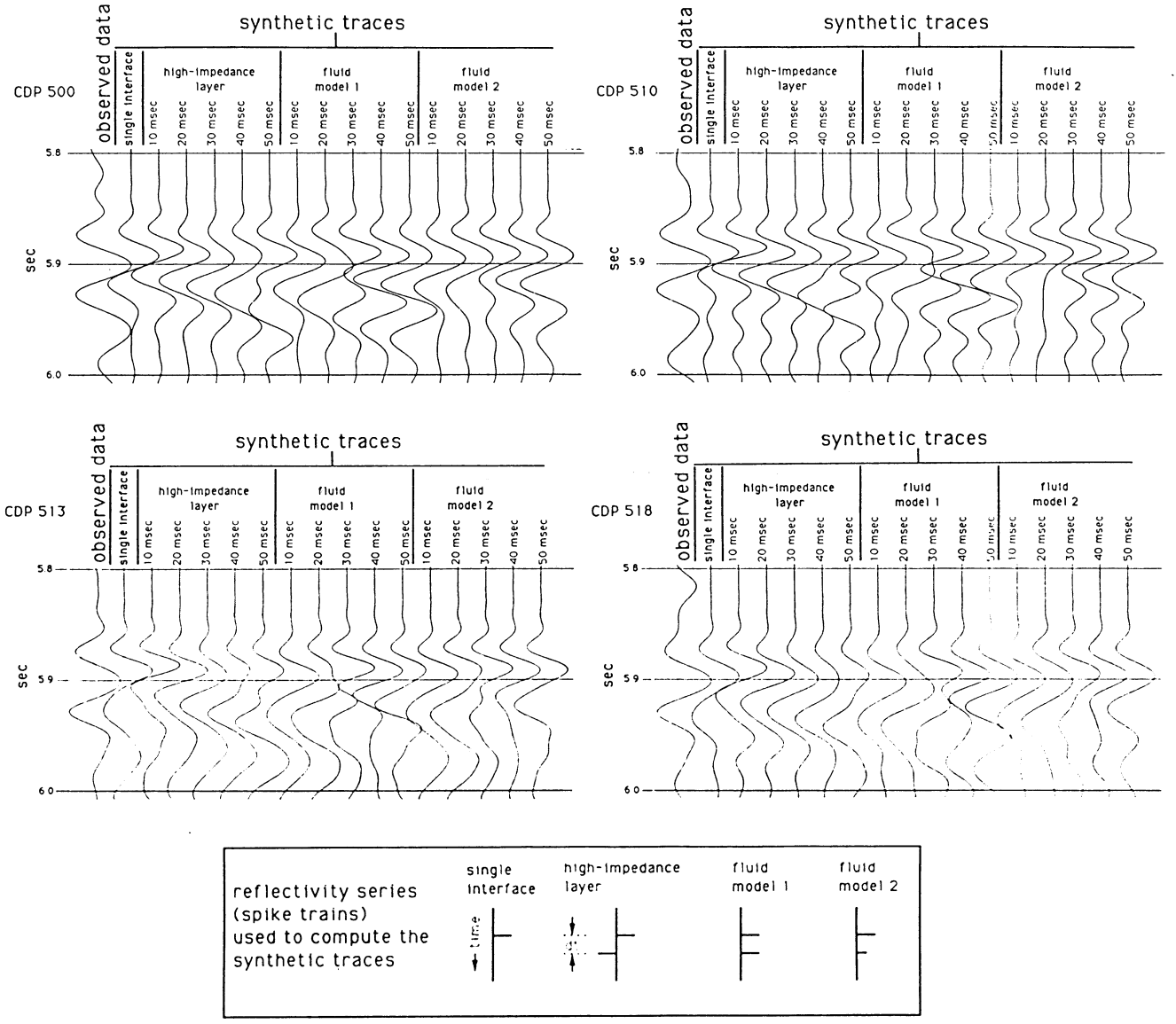

Fig. 12. Modeling results for four representative CDPs showing the SBS on observed data along with synthetic traces representing the reflection from a single-interface, a high-impedance layer, and two fluid-filled porous zones. The times above the three latter models represent the two-way transit time through a range of layer thicknesses. The box at the bottom shows the reflectivity functions (reflection coefficient versus time) for each of the models. See text for further explanation of the models. Traces are scaled to equalize the maximum amplitude of each trace.

vibroseis models. Given the nearly equal positive and negative lobes on the source wavelets (Figure 9*b*), this tuning would produce a wavelet package with an apparent amplitude nearly double that of the component reflections. Obviously the lower amplitude of the bottom reflector complicates this otherwise simple model, but, as mentioned above, the presence of several thin mafic bodies or a shear zone could make the lower boundary appear less reflective.

Constructive interference is not as effective with the 54 ms reflector separation in the fluid model, but it is well known that fluid and gas-filled porous zones can produce very large reflection coefficients even without wavelet tuning [e.g., *Koefoed*, 1955; *Domenico*, 1974; *Ensley*, 1984]. The main drawback we see to this model is the lack of a reflection from the top of the porous zone. This constrains the SBS to have a well defined lower boundary to the porous zone, two fluids with largely different physical properties, and a diffuse upper boundary. The two-fluid requirement is a particularly stringent constraint given that the existence of any free fluid at 16 km depth is debateable [e.g., *Yardley*, 1986]. While these constraints do not preclude the fluid hypothesis, its complexity contrasts sharply with the simple high-impedance model. We must keep in mind, however, that the SBS is an unusually bright reflection and could therefore be the result of an unusual set of conditions.

The SBS is not the only such reflector in the area, it is merely the brightest. Within the zone of dipping reflectors which delineate the interpreted late Paleozoic suture there are at least three other bright reflections (one is visible at 5.0 s traveltime on the left edge of Figure 1) which presumably have the same origin as the SBS. The SBS stands out from the other reflectors in part because it has two geometric characteristics which enhance its reflection amplitude: its thickness is tuned to increase the reflection amplitude, and it is extremely level along much of its length so the reflected energy is directed upward to the geophone array.

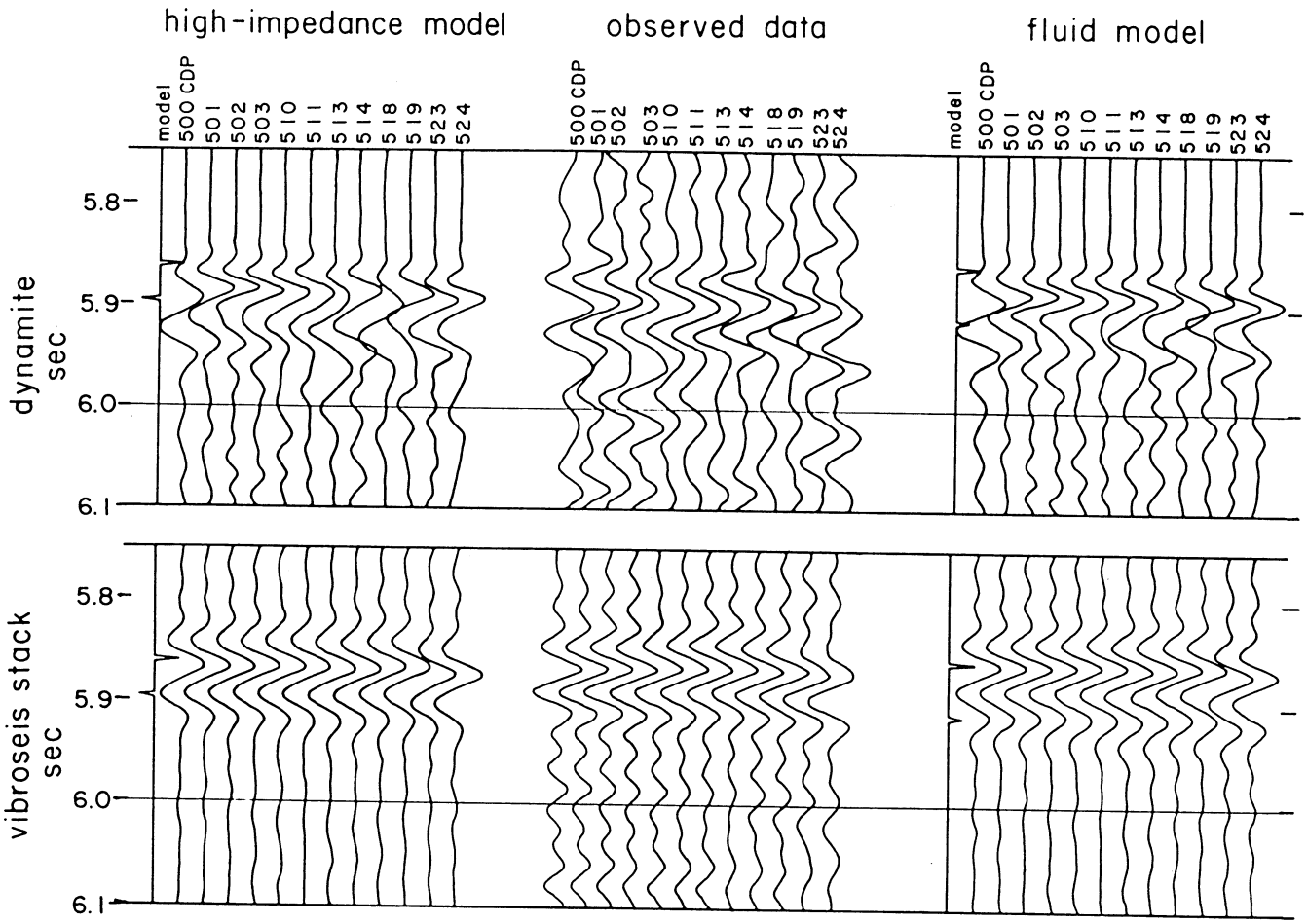

Fig. 13. Comparison of the observed dynamite (top center) and vibroseis stacked data (bottom center) with our best high-impedance model (left) and fluid-filled porous zone model (right). The high-impedance model has a 36 ms two-way transit time through the layer and reflection coefficients of +1.0 and -0.7 for the top and bottom of the layer. The fluid model has a 54 ms two-way transit time and reflection coefficients of +1.0 and +0.5 at the top and bottom of the layer. Traces are scaled to equalize the maximum amplitude of each trace.

Though these characteristics may be fortuitous, they are by no means improbable.

A likely candidate for the SBS body is that it is part of the suite of Mesozoic-aged diabase sills and dikes which are widespread in the region [*McBride et al.*, 1989; *Ragland et al.*, 1983]. If so, the location within the late Paleozoic suture may be related to the emplacement of magma within pre-existing weaknesses reopened during Mesozoic time. However, a small mafic or ultramafic body tectonically emplaced during the late Paleozoic collision is an equally viable alternative.

This is at least the third location at which strong reflections within crystalline basement rocks have been shown to likely originate from thin mafic intrusions. At the Siljan impact structure in Sweden, drilling has confirmed that at least three strong, continuous reflectors imaged on seismic reflection data are caused by dolerite dikes [*Juhlin*, 1987]. The Bagdad Reflection Sequence of the western U.S. [*Hauser et al.*, 1987], a set of reflections very much like those at Siljan [*Goodwin et al.*, 1989; *Litak and Hauser*, 1991], are almost certainly mafic dikes because modeling of the individual reflections as thin, high-impedance layers produces an excellent match with observed data [*Goodwin et al.*, 1989] and modeling the reflections as a series of thin mafic dikes like those exposed in the nearby Buck mountains produces a very similar seismic section [*Litak and Hauser*, 1991]. That these suites of mafic intrusions cause prominent reflections is no surprise; the widespread occurrence of such intrusives suggest that they will be one of the major causes of reflectivity in crystalline rocks as we continue to explore the continents [e.g., *MacDonald*, 1988].

COCORP returned to the SBS in the summer of 1990 for a more rigorous test of the fluid hypothesis and to determine how well the seismic technique can distinguish the physical properties of deep reflectors. The experiment used both compressional and shear-wave expanding spread profiles (ESPs). Shear-waves can elicit a markedly different reflection response from a porous zone [e.g., *Ensley*, 1984; *Robertson and Pritchett*, 1985] and could therefore prove crucial in confirming the cause of middle or lower crustal reflections if the source energy can penetrate to those depths. In particular, a mafic intrusive would be expected to have approximately the same reflection coefficient on both P- and S-wave data, whereas a porous zone filled with a gas or fluid may not [e.g., *Robertson and Pritchett*, 1985]. Furthermore, the ESPs will likely show a markedly different response if a porous zone is present than if a mafic intrusive is present [*Koefoed*, 1955; *Ostrander*, 1984]. ESPs have been widely used to determine the cause of reflections in the shallow crust, with some workers even claiming that the technique can distinguish between different pore fluids [e.g., *Yu*, 1985]. Assuming the shear-wave energy penetrated the ~1.5 km of Atlantic Coastal Plain sedimentary

rocks, the SBS should be a good testing ground for middle and lower crustal shear-wave applications because of its isolated location in what appear to be seismically efficient crystalline rocks.

CONCLUSIONS

An analysis of both explosion and vibroseis data acquired over the Surrency Bright Spot (SBS) shows that it has a positive reflection coefficient at or near its upper surface. Waveform modeling demonstrates that two or more thinly spaced reflectors contribute to the returning waveform. A simple, roughly 120 m thick high impedance layer, with a positive reflection at its upper boundary and a slightly smaller negative reflection coefficient at its base, provides a very good match to the observed data when modeled. Though the lower boundary must differ slightly from the upper, such a model could represent a mafic intrusion or thin ultramafic sliver, either of which could produce appropriate reflection coefficients. A fluid-filled porous zone model based on analogies with "flat spots" seen on shallow seismic sections, modeled as two positive reflectors marking a fluid-fluid interface within a porous zone and the base of the porous zone, seems plausible. The fluid model, however, must involve two fluids, have a relatively nonreflective upper boundary to the porous zone, and the lower liquid must fill a zone about 150 m in thickness. The high-impedance layer provides the simpler explanation, but the fluid hypothesis is not disproved by this experiment.

Acknowledgments. Funding for the data acquisition was provided by BP Exploration and the National Science Foundation. Amoco Production Company generously donated equipment and substantial personnel time to the study. We thank John Myers of Amoco Production Company in particular for his efforts in the field. The experiment took place on the property of the Union Camp Corporation who kindly allowed us to freely roam their property. Data processing was done primarily on the Cornell Theory Center's IBM 3090-600E computers at the Cornell National Supercomputer Facility. Greg Steiner, Bob Smalley, and Jer-Ming Chiu of the University of Tennessee, Memphis, provided some of the monitoring equipment as well as instruction on its usage. Steve Gallow, Kathleen Vargason, and Jane Axemathy provided technical assistance. The paper has benefited from discussions with Art Barnes, Larry Brown, Sid Kaufman, Doug Nelson, and Jack Oliver at Cornell. Tom Brocher, Ron Clowes, and Dave Okaya provided thoughtful reviews of the manuscript. The Consortium for Continental Reflection Profiling (COCORP) is supported by National Science Foundation grant EAR-8916129. Institute for the Study of the Continents (INSTOC) contribution 142.

REFERENCES

Ake, J.P., and A.R. Sanford, New evidence for the existence and internal structure of a thin layer of magma at mid-crustal depths near Socorro, New Mexico, *Bull. Seismol. Soc. Am., 78*, 1335-1359, 1988.

Akima, H., A new method of interpolation and smooth curve fitting based on local procedures, *J. Assoc. Comput. Mach., 17*, p. 589-602, 1970.

Almoghrabi, H., and J. Lange, Layers and bright spots, *Geophysics, 51*, 699-709, 1986.

Backus, and Chen, Flat-spot exploration, *Geophys. Prospect., 23*, 533-577, 1975.

Bailey, R.C., J.A. Craven, J.C. Macnae, and B.D. Polzer, Imaging of fluids in Archean crust, *Nature, 340*, 136-138, 1989.

Brown, L.D., D. Wille, L. Zheng, B. deVoogd, J. Mayer, T. Hearn, W. Sanford, C. Caruso, T.-F. Zhu, K.D. Nelson, C. Potter, E. Hauser, S. Klemperer, S. Kaufman, and J. Oliver, COCORP: new perspectives on the deep crust, *Geophys. J., 89*, 47-54, 1987.

Brown, L.D., C.E. Chapin, A.R. Sanford, S. Kaufman, and J.E. Oliver, Deep structure of the Rio Grande Rift from seismic reflection profiling, *J. Geophys. Res., 85*, 4773-4800, 1980.

Carlson, R. L., and C.N. Herrick, Densities and porosities in the oceanic crust and their variations with depth and age, *J. Geophys. R.,95*, 9153-9170, 1990.

Claerbout, J.F., Fundamentals of Geophysical Data Processing, 274 pp. McGraw-Hill, New York, 1976.

deVoogd, B., L. Serpa, and L.D. Brown, Crustal extension and magmatic processes: COCORP profiles from Death Valley and the Rio Grande rift, *Geol. Soc. Am. Bull., 100*, 1550-1567, 1988.

Domenico, S.N., Effect of water saturation on seismic reflectivity of sand reservoirs encased in shale, *Geophysics, 39*, 759-769, 1974.

Ensley, R.A., Comparison of P- and S-wave seismic data: A new method for detecting gas reservoirs, *Geophysics, 49*, 1420-1431, 1984.

Frost, B.R., W.S. Fyfe, K. Tazaki, and T. Chan, Grain-boundary graphite in rocks and implication for high electrical conductivity in the lower crust, *Nature, 340*, 134-136, 1989.

Fyfe, W.S., Fluids in deep continental crust, in Reflection Seismology: The Continental Crust, edited by M. Barazangi and L. Brown, *Geodyn. Ser. 14*, pp. 33-40, AGU, Washington, D.C., 1986.

Gardner, G.H.F, L.W. Gardner, and A.R. Gregory, Formation velocity and density - the diagnostic basics for stratigraphic traps, *Geophysics, 39*. 770-780, 1974.

Goodwin, E.B., G.A. Thompsen, and D.A. Okaya, Seismic identification of basement reflectors: the Bagdad reflection sequence in the Basin and Range province-Colorado Plateau transition zone, Arizona, *Tectonics, 8*, 821-831, 1989.

Gough, D.I., Seismic reflectors, conductivity, water and stress in the continental crust, *Nature, 323*, 143-144, 1986.

Gregory, A.R., Fluid saturation effects on dynamic elastic properties of sedimentary rocks, *Geophysics, 41*, 895-921, 1976.

Hauser, E.C., J. Gephart, T. Latham, J.E. Oliver, S. Kaufman, L.D. Brown, and I. Lucchitta, COCORP Arizona transect: Strong crustal reflections and offset Moho beneath the transition zone, *Geology, 5*, 1103-1106, 1987.

Hurich, C.A., and S.B. Smithson, Compositional variation and the origin of deep crustal reflections, *Earth Planet. Sci. Lett., 85*, 416-426, 1987.

Hyndman, R.D., and D.W. Hyndman, Water saturation and high electrical conductivity in the lower continental crust, *Earth Planet. Sci. Lett., 4*, 427-432, 1968.

Hyndman, R.D., and P.M. Shearer, Water in the lower continental crust: modelling magnetotelluric and seismic reflection results, *Geophys. J. Int., 98*, 343-365, 1989.

Juhlin, C., Interpretation of the seismic reflectors in the Gravberg-1 well, in Deep drilling in crystalline bedrock, edited by A. Boden, and K.G. Eriksson, Springer-Verlag, Berlin, pp. 113-121, 1988.

Koefoed, O., On the effect of Poisson's ratio of rock strata on the reflection coefficients of plane waves, *Geophys. Prospect., 3*, 381-387, 1955.

Koslovsky, Y.A., The world's deepest well, *Sci. Am., 251*, (6), 98-104, 1984.

Litak, R.K., and E.C. Hauser, Mafic intrusions and strong crustal reflections: Seismic modelling of the Bagdad reflection sequence, Arizona, *Geol. Soc. Am. Bull.*, in press, 1991.

Luschen, E., F. Wenzel, K.-J. Sandmeier, D. Menges, Th. Ruhl, M. Stiller, W. Janoth, F. Keller, W. Sollner, R. Thomas, A. Krohe, R. Stenger, K. Fuchs, H. Wilhelm, and G. Eisbacher, Near-vertical and wide-angle seismic surveys in the Black Forest, SW Germany, *J. Geophys., 62*, 1-30, 1987.

MacDonald, G.J., Major questions about deep continental structures, in Deep drilling in crystalline bedrock, edited by A. Boden, and K.G. Eriksson, Springer-Verlag, Berlin, pp. 28-48, 1988.

Matthews, D.H., and M.J. Cheadle, Deep reflections from the Caledonides and Variscides west of Britain and comparison with the Himalayas, in Reflection Seismology: A Global Perspective, Geodyn. Ser., 13, edited by M. Barazangi, and L.D. Brown, pp. 5-19, 1986.

McBride, J.H., K.D. Nelson, and L.D. Brown, Evidence and implications of an extensive early Mesozoic rift basin and basalt/diabase sequence beneath the southeast coastal plain, *Geol. Soc. Am. Bull., 101*, 512-520, 1989.

Nelson, K.D., J.A. Arnow, J.H. McBride, J.H. Willemin, J. Huang, L. Zheng, J.E. Oliver, L.D. Brown, and S. Kaufman, New COCORP profiling in the southeastern United States. Part I: Late Paleozoic suture and Mesozoic rift basin, *Geology, 13*, 714-718, 1985.

Ostrander, W.J., Plane-wave reflection coefficients for gas sands at nonnormal angles of incidence, *Geophysics, 49*, 1637-1648, 1984.

Ragland, P.C., R.D. Hatcher, Jr., and D. Whittington, Juxtaposed Mesozoic diabase dike sets from the Carolinas: a preliminary assessment, *Geology*, *11*, 394-399, 1983.

Robertson, J.D., and W.C. Pritchett, Direct hydrocarbon detection using comparative P-wave and S-wave seismic sections, *Geophysics*, *50*, 383-393, 1985.

Robinson, E.A., and S. Treitel, Geophysical Signal Analysis, 466 pp., Prentice-Hall, Englewood Cliffs, N.J., 1980.

Shankland, T.J., A case of two conductors, *Nature*, *340*, 102, 1989.

Warner, M.R., Basalts, water, or shear zones in the lower continental crust?, *Tectonophysics*, *173*, 163-174, 1990.

White, R.E., and P.N.S. O'Brien, Estimation of the primary seismic pulse, *Geophys. Prospect.*, *22*, 627-651, 1974.

Widess, M.B., How thin is a thin bed?, *Geophysics*, *38*, 1176-1180, 1973.

Wille, D.M., The COCORP Surrency bright spot: fluid in the deep crust?, M.S. thesis, 46 pp., Cornell Univ., Ithaca, N.Y., 1987.

Yardley, B.W.D., Is there water in the deep continental crust?, *Nature*, *323*, 111, 1986.

Yilmaz, O., Seismic Data Processing, 526 pp. Society of Explorations Geophysicists, Tulsa, Oklahoma, 1987.

Yu, G., Offset-amplitude variation and controlled-amplitude processing, *Geophysics*, *50*, 2697-2708, 1985.

T.L. Pratt, U.S. Geological Survey, MS 966, Box 25046, Denver Federal Center, Denver, CO 80225-0046.

E.C. Hauser, Institute for the Study of the Continents, Snee Hall, Cornell University, Ithaca, NY 14853-1504.

T.M. Hearn, Department of Physics, New Mexico State University, Las Cruces, NM 88003-0001.

T.J. Reston, GEOMAR, Wischhofstrasse 1-3, 2300 Kiel, Germany.

(Received April 9, 1990;
revised August 6, 1990;
accepted August 8, 1990.)